

EUROPEAN ORGANISATION FOR NUCLEAR RESEARCH (CERN)



Submitted to: Physical Review D

CERN-EP-20XX-XXX
June 4, 2020

Search for an exotic $S=-2$, $Q=-2$ baryon resonance in proton-proton interactions at $\sqrt{s_{NN}} = 17.3$ GeV

The NA61/SHINE Collaboration

Pentaquark states have been extensively investigated theoretically in the context of the constituent quark model. In this paper results of an experimental search for pentaquarks in the $\Xi^- \pi^-$, $\Xi^- \pi^+$, $\Xi^+ \pi^-$ and $\Xi^+ \pi^+$ invariant mass spectra in proton-proton interactions at $\sqrt{s}=17.3$ GeV are presented. Previous possible evidence from the NA49 collaboration of the existence of a narrow $\Xi^- \pi^-$ baryon resonance in p+p interactions is not confirmed with almost 10 times greater event statistics. The search was performed using the NA61/SHINE detector which reuses the main components of the NA49 apparatus. No signal was observed with either the selection cuts of NA49 or newly optimised cuts.

1 Introduction

During the past decades pentaquark states have been extensively investigated theoretically in the context of the constituent quark model [1, 2, 3, 4]. Some of these states are proposed to be closely bound and to have charge and strangeness quantum number combinations that cannot be realized as three-quark states. Using the chiral soliton model an anti-decuplet of baryons was predicted by Chemtob [5]. The lightest member was estimated by Praszalowicz [6] to lie at a mass of 1530 MeV. Diakonov et al. [7] subsequently derived a width of less than 15 MeV for this exotic baryon resonance state $\Theta^+(1540)$ ($uudd\bar{s}$), with $S = +1$, $J^P = \frac{1}{2}^+$. They further made predictions for the heavier members of the anti-decuplet, with the isospin quartet of $S = -2$ baryons having a mass of about 2070 MeV and partial decay width into $\Xi\pi$ of about 40 MeV. This isospin $\frac{3}{2}$ multiplet contains two $\Xi_{3/2}$ with ordinary charge assignments ($\Xi_{3/2}^0, \Xi_{3/2}^-$) in addition to the exotic states $\Xi_{3/2}^+$ ($uuss\bar{d}$) and $\Xi_{3/2}^{--}$ ($ddss\bar{u}$). The $\Xi_{3/2}$ isospin quartet has also been discussed as a part of higher multiplets. Jaffe and Wilczek [8] on the other hand based their predictions on the strong color-spin correlation force and suggest that the $\Theta^+(1540)$ baryon is a bound state of two highly correlated ud pairs and an antiquark. In their model the $\Theta^+(1540)$ has positive parity and lies in an almost ideally mixed $\overline{10}_f \oplus 8_f$ multiplet of $SU(3)_f$. For the isospin $\frac{3}{2}$ multiplet of Ξ s they predict a mass around 1750 MeV and a width 50% greater than that of the $\Theta^+(1540)$. For the theoretical and experimental status of these low-mass multi-quark states see e.g. Ref. [9].

Experimentally, since the first observation of a $\Theta^+(1540)$ candidate [10], there is still a lack of consensus about whether the lightest member of the exotic anti-decuplet has been discovered. After about fifteen years of excitement the results are still controversial. There are numerous reports from different groups that conducted searches for Θ^+ with some observing a signal and while others observing a null result, for review see Refs. [9, 11]. The reason why some experiments see Θ^+ , while the others do not, may be either of experimental nature or a peculiar production mechanism (or both).

Observation of candidates for the heaviest members of the $\overline{10}$ multiplet was reported only by the NA49 experiment in p+p reactions at CERN [12]. This result was not confirmed by other experiments (see e.g. Refs. [13, 14]), however, in different reactions and phase space regions. For a fuller review of the available experimental results again see Ref. [9].

An extensive program of investigation of pentaquark states containing c or b quarks and having masses above 4000 MeV is being pursued at many accelerators. Numerous candidates, including the ones observed recently by the LHCb experiment [15, 16], were found and confirmed, see e.g. Ref. [11] for a recent review.

The NA61/SHINE experiment at the CERN SPS essentially reuses the detector of NA49 with upgrades allowing a factor 10 higher data recording rate. This paper discusses the experimental search for the existence of the exotic $\Xi_{3/2}^{--}$ member of the Ξ multiplet employing the same detector with the same acceptance, similar analysis techniques, in the same reaction and at the same center-of-mass energy as studied by the NA49 experiment, but with 10 times greater events statistics. The results of the search for the $\Xi_{3/2}^{--}$ and $\Xi_{3/2}^0$ states and their antiparticles in proton-proton interactions at $\sqrt{s} = 17.3$ GeV are presented and compared to the published data of NA49.

2 The NA61/SHINE detector

Data used for the analysis reported here were recorded at the CERN SPS accelerator complex with the NA61/SHINE fixed target large acceptance hadron detector [17], which inherited most of the apparatus from NA49. The NA61/SHINE tracking system consists of 4 large volume time projection chambers (TPCs). Two of the TPCs (VTPC1 and VTPC2) are within superconducting dipole magnets. Downstream of the magnets two larger TPCs (MTPC-R and MTPC-L) provide acceptance at high momenta. The interactions were produced with a beam of 158 GeV/c protons on a cylindrical liquid hydrogen target of 20 cm length and 2 cm transverse diameter.

3 Analysis

The recorded data sample consists of about 53M events. Reconstruction started with pattern recognition, momentum fitting, and finally formation of global track candidates. These track candidates generally spanned multiple TPCs and consisted of charged particles produced in the primary interaction and at secondary vertices. The primary vertex was determined for each event. Events in which no primary vertex was found were rejected. To remove non-target interactions, the reconstructed primary vertex was required to lie within the target; ± 9 cm in the longitudinal (z) direction, and within ± 1 cm in the transverse (x, y) direction from the geometric center of the target. These cuts reduced the data sample to 33M inelastic p+p interactions. Particle identification was performed via measurement of the specific energy loss (dE/dx) in the TPCs. The achieved resolution is 3–6% depending on the reconstructed track length [17, 18]. The dependence of the measured dE/dx on velocity was fitted to a Bethe-Bloch type parametrisation.

The first step in the analysis was the search for Λ candidates, which were then combined with the π^- to form the Ξ^- candidates. Next, the $\Xi_{3/2}^{--}$ ($\Xi_{3/2}^0$) were searched for in the $\Xi^- \pi^-$ ($\Xi^- \pi^+$) invariant mass spectrum, where the π^- (π^+) are primary vertex tracks. An analogous procedure was followed for the antiparticles.

The Λ candidates are formed by pairing reconstructed and identified tracks with appropriate mass assignments and opposite charge. These particles are tracked backwards through the NA61/SHINE magnetic field from the first recorded point, which is required to lie in one of the VTPC detectors. This backtracking is performed in 2 cm steps in the z (beam) direction. At each step the separation in the transverse coordinates x and y is evaluated and a minimum is checked for. A pair is considered a Λ candidate if the distance of closest approach in the x and y direction is below 1 cm in both directions. Using the distances at the two neighbouring space points around the point of closest approach, a more accurate Λ position is found by interpolation. This position, together with the momenta of the tracks at this point, are used as the input for a 9 parameter fit using the Levenberg-Marquardt fitting procedure [19].

Ξ^- candidates were assembled by the combination of all π^- with those Λ candidates having a reconstructed invariant mass within ± 15 MeV of the nominal PDG [20] mass. A fitting procedure is applied using as parameters the decay position of the V^0 candidate, the momenta of both the V^0 decay tracks, the momentum of the daughter track, and finally the z position of the Ξ^- decay point. The x and y coordinates of the Ξ decay position are not subject to the minimization, as they are determined from the parameters using momentum conservation. This procedure yields the decay position and the momentum of the Ξ^- candidate.

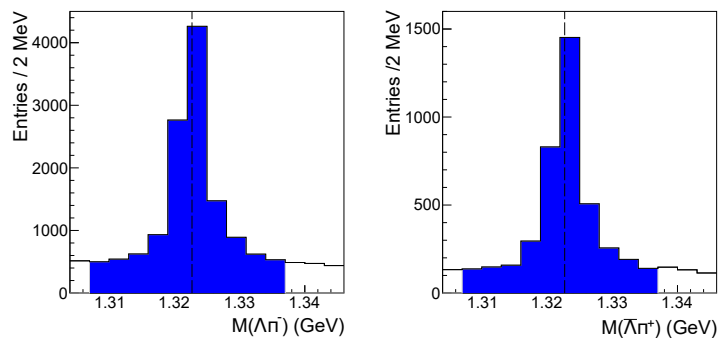


Figure 1: (Color online) The $\Lambda\pi^-$ invariant mass spectrum of Ξ^- candidates (*left panel*). Filled areas indicate the mass range of the selected candidates. The vertical dashed black line shows the nominal PDG Ξ mass. Analogous $\Lambda\pi^+$ invariant mass spectrum of Ξ^+ candidates (*right panel*).

Specific cuts were imposed to increase the significance of the Ξ^- signal. As the combinatorial background is concentrated close to the primary vertex, a distance cut of > 12 cm between the primary and the Ξ^- vertex was applied. Additional cuts on extrapolated track impact parameters in the x (magnetic bending) and y (non-bending) directions (b_x and b_y) at the primary vertex were imposed. To ensure that the Ξ^- originates from the primary vertex, its $|b_x|$ and $|b_y|$ were required to be less than 2 cm and 1 cm, respectively. On the other hand, the π^- from the Ξ^- decay were required to have $|b_y| > 0.2$ cm. The resulting $\Lambda\pi^-$ invariant mass spectrum is shown in Fig. 1 (*left*), where the Ξ^- peak is clearly visible. The Ξ^- candidates were selected within ± 15 MeV of the nominal Ξ^- mass. Only events with one Ξ^- candidate (95%) were retained. Exactly the same procedure was applied for antiparticles, resulting in the Ξ^+ peak shown in Fig. 1 (*right*).

To search for the exotic $\Xi_{3/2}^{--}$ the selected Ξ^- candidates were combined with primary π^- tracks. To select π^- from the primary vertex, their impact parameter $|b_y|$ was required to be less than 0.5 cm and their dE/dx be within 2.5σ of their nominal Bethe-Bloch value. All cuts were optimized to maximize the signal-to-background ratio of the mass peaks of the $\Xi(1530)$, which decays into the channel where the pentaquark candidates with ordinary charge assignment may be observed. Moreover, to increase the signal-to-background ratio in the region of the $\Xi(1530)$, an additional $\theta > 1^\circ$ cut was applied, with θ being the opening angle between the Ξ^- and the π^- in the laboratory frame. All $\Xi\pi$ combinations were analysed following the same procedure. The resulting $\Xi^- \pi^-$, $\Xi^- \pi^+$, $\Xi^+ \pi^-$ and $\Xi^+ \pi^+$ invariant mass spectra are shown in Fig. 2 (*left*).

Additionally, a second set of more stringent selection criteria was implemented following exactly the procedure of the NA49 experiment in which possible evidence of the existence of the $\Xi_{3/2}^{--}$ was found [12]: the Ξ^- was required to have $|b_x| < 1.5$ cm and $|b_y| < 0.5$ cm at the primary vertex, the π^- from the Ξ^- decay $|b_y| > 0.5$ cm at the primary vertex, and the selected π^- from the primary vertex $|b_x| < 1.5$ cm and $|b_y| < 0.5$ cm. Moreover, the dE/dx had to be within 1.5σ of the nominal Bethe-Bloch value. The restriction on the opening angle between the Ξ^- and the π^- in the laboratory frame was $\theta > 4.5^\circ$. In addition to the described cuts, a lower cut of 3 GeV/c was imposed on the π^+ momenta to minimize proton contamination (the cut reduces the range of acceptance at small invariant mass and therefore the $\Xi(1530)$ signal disappears in the $\Xi^- \pi^+$ mass distribution). The resulting $\Xi^- \pi^-$, $\Xi^- \pi^+$, $\Xi^+ \pi^-$, and $\Xi^+ \pi^+$ invariant mass spectra with NA49 selection criteria are shown in Fig. 2 (*right*).

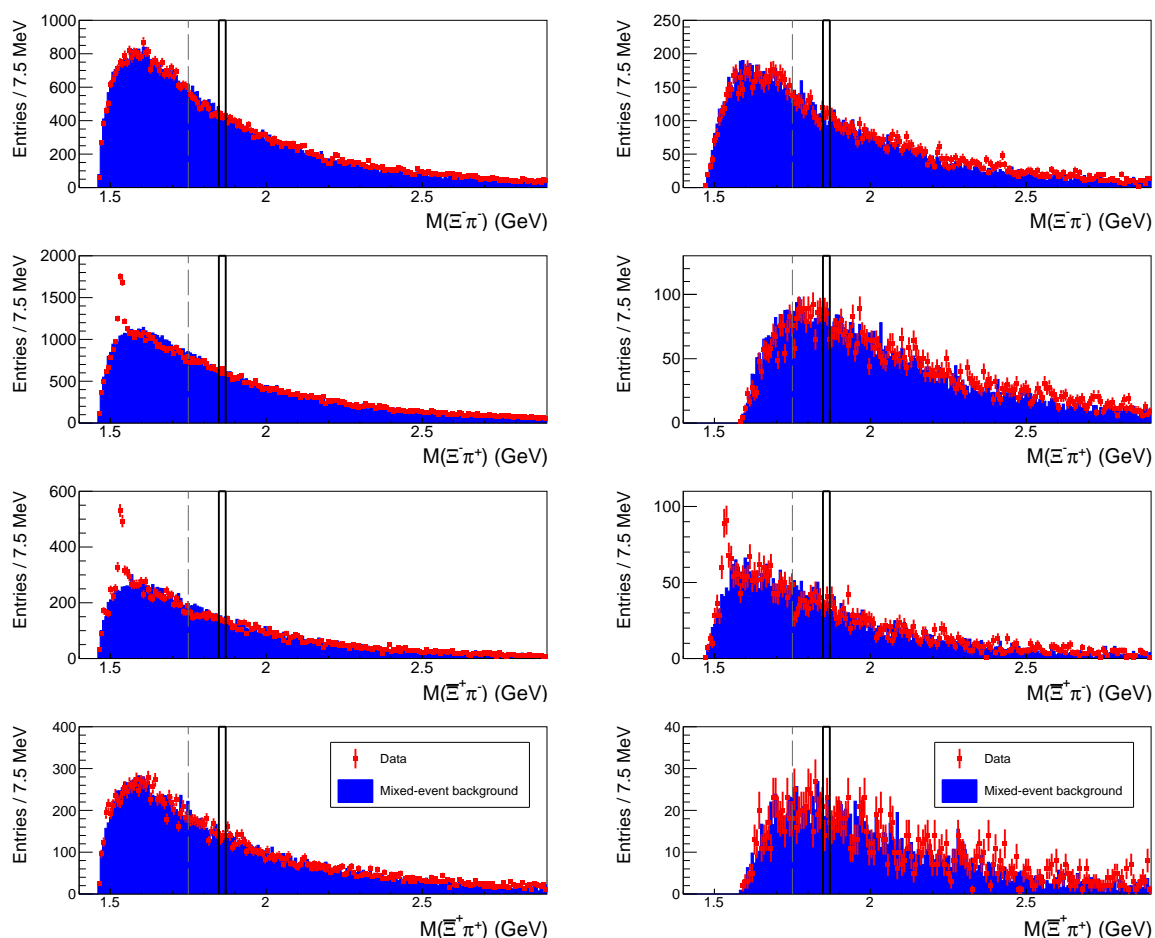


Figure 2: (Color online) Invariant mass spectra of $\Xi^- \pi^-$, $\Xi^- \pi^+$, $\Xi^+ \pi^-$, $\Xi^+ \pi^+$ combinations after selection criteria optimized to maximize the signal to background ratio of the $\Xi(1530)$ (*left*) and after selection cuts following exactly the procedure of the NA49 experiment where possible evidence of the existence of $\Xi_{3/2}^-$ was found (*right*). The filled histograms are the normalised mixed-event background. The vertical dashed gray line shows the theoretically predicted $\Xi_{3/2}^-$ mass from the model of Ref. [8]. The black rectangle indicates the mass window in which the NA49 collaboration has seen an enhancement with significance up to 4.0 standard deviations. A narrow peak of the $\Xi(1530)^0$ state is observed in the invariant mass spectra of $\Xi^- \pi^+$ and of $\Xi^+ \pi^-$.

4 Results

The invariant mass distributions of $\Xi^- \pi^-$, $\Xi^- \pi^+$, $\Xi^+ \pi^-$, $\Xi^+ \pi^+$ combinations measured by NA61/SHINE are plotted in Fig. 2. The filled histograms show the mixed-event background normalised to the number of real combinations. The vertical dashed gray line shows the theoretically predicted $\Xi_{3/2}^-$ mass from the model discussed in Ref. [8]. The black rectangle indicates the mass window in which the NA49 collaboration has seen an enhancement with significance up to 4.0 standard deviations. For completeness, the sum of the four mass distributions is displayed in Fig. 3 for both sets of cuts. For the combined distributions NA49 reported an observed signal significance of 5.6 standard deviations. Independently of the implemented strategy of the signal-to-background optimization, the data is consistent with the mixed-event background in the mass window around the theoretical predictions of the $\Xi_{3/2}^-$ mass. No signal from

$\Xi_{3/2}^{--}$, $\Xi_{3/2}^0$ states, and their antiparticles is observed in all invariant mass distributions.

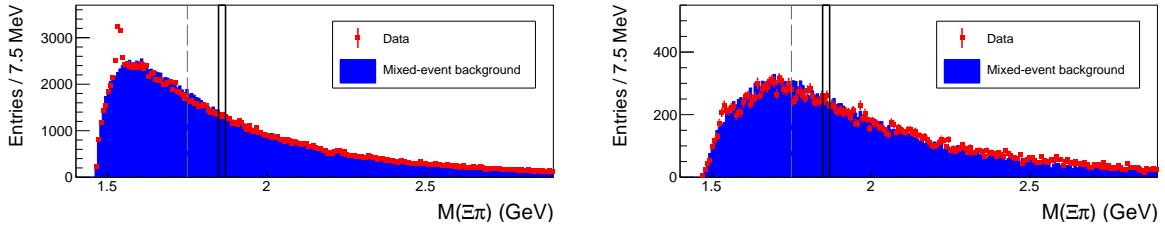


Figure 3: (Color online) The sum of the $\Xi^- \pi^-$, $\Xi^- \pi^+$, $\Xi^+ \pi^-$, and $\Xi^+ \pi^+$ invariant mass spectra after selection criteria optimized to maximize the signal-to-background ratio of the $\Xi(1530)$ (*left*), and after selection cuts following exactly the procedure of the NA49 experiment (*right*). The filled histograms are the normalised mixed-event background. The vertical dashed gray line shows the theoretically predicted $\Xi_{3/2}^{--}$ mass from the model of Ref. [8]. The black rectangle indicates the mass window in which the NA49 collaboration observed an enhancement with significance of 5.6 standard deviations. A narrow peak of the $\Xi(1530)^0$ state is observed.

The sensitivity of the results to variations of the different cuts and event selection criteria was investigated by varying the dE/dx cut used for particle selection, by changing the width of accepted regions around the nominal Ξ^- and Λ masses, by investigating different event topologies (e.g. the number of π mesons per event), by selecting tracks with different number of clusters, as well as by using different b_x and b_y cuts. Furthermore, the influence of resonances (including the possibility of particle misidentification) which could affect the signal was checked. In all cases no signal of $\Xi_{3/2}^{--}$ emerged.

A narrow peak of the known $\Xi(1530)^0$ state [20] is observed in the invariant mass distribution of $\Xi^- \pi^+$ for selection criteria optimized to maximize the signal to background ratio of the $\Xi(1530)$, and of $\Xi^+ \pi^-$ for both selection criteria. The measured mass of $\Xi(1530)^0$ (1534 ± 3 MeV) is consistent with PDG, while the yield scales appropriately with the number of events when comparing to NA49 results (using the NA49 selection criteria).

Figure 4 shows the background-subtracted sum of the four invariant mass distributions displayed in Fig. 3 (*right*). Superimposed is a similar (Fig. 3b in Ref. [12]) distribution observed by NA49 renormalized to the same number of selected p+p interactions.

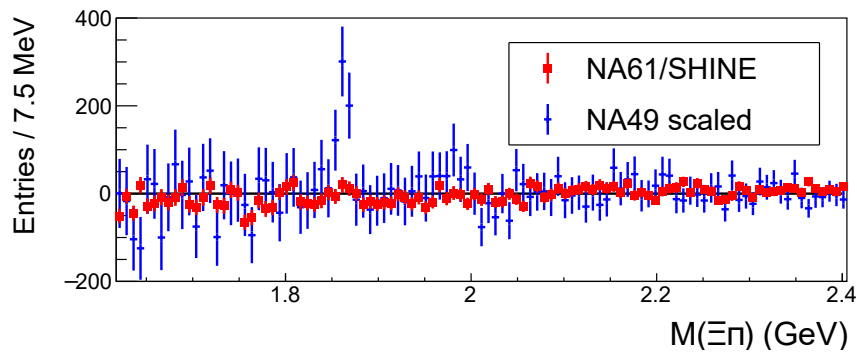


Figure 4: (Color online) The background-subtracted sum of the $\Xi^- \pi^-$, $\Xi^- \pi^+$, $\Xi^+ \pi^-$, and $\Xi^+ \pi^+$ invariant mass spectra after selection cuts following exactly the procedure of the NA49 experiment. The red squares are the NA61/SHINE data, the blue points correspond to the renormalized NA49 distribution (Fig. 3b in Ref. [12]) in which a narrow peak with significance of 5.6 standard deviations is visible.

In conclusion, the NA61/SHINE analysis of p+p interactions at $\sqrt{s}=17.3$ GeV with 10 times greater

statistics compared to the NA49 analysis [12] does not show any indication of narrow $\Xi_{3/2}^{--}$, $\Xi_{3/2}^0$, $\Xi_{3/2}^{++}$, $\Xi_{3/2}^0$ states. No signal is observed in invariant mass distributions of $\Xi^- \pi^-$, $\Xi^- \pi^+$, $\Xi^+ \pi^-$, and $\Xi^+ \pi^+$. This is particularly true for the mass window (1848 - 1870 MeV) in which the NA49 collaboration had seen an enhancement with significance up to 5.6 standard deviations.

Acknowledgments

We would like to thank the CERN EP, BE, HSE and EN Departments for the strong support of NA61/SHINE.

This work was supported by the Hungarian Scientific Research Fund (grant NKFIH 123842/123959), the Polish Ministry of Science and Higher Education (grants 667/N-CERN/2010/0, NN 202 48 4339 and NN 202 23 1837), the National Science Centre Poland (grants 2011/03/N/ST2/03691, 2013/11/N/ST2/03879, 2014/13/N/ST2/02565, 2014/14/E/ST2/00018, 2014/15/B/ST2/02537 and 2015/18/M/ST2/00125, 2015/19/N/ST2 /01689, 2016/23/B/ST2/00692, 2017/25/N/ST2/02575, 2018/30/A/ST2/00226), the Russian Science Foundation, grant 16-12-10176, the Russian Academy of Science and the Russian Foundation for Basic Research (grants 08-02-00018, 09-02-00664 and 12-02-91503-CERN), the Ministry of Science and Education of the Russian Federation, grant No. 3.3380.2017/4.6, the National Research Nuclear University MEPhI in the framework of the Russian Academic Excellence Project (contract No. 02.a03.21.0005, 27.08.2013), the Ministry of Education, Culture, Sports, Science and Technology, Japan, Grant-in-Aid for Scientific Research (grants 18071005, 19034011, 19740162, 20740160 and 20039012), the German Research Foundation (grant GA 1480/2-2), the Bulgarian Nuclear Regulatory Agency and the Joint Institute for Nuclear Research, Dubna (bilateral contract No. 4799-1-18/20), Bulgarian National Science Fund (grant DN08/11), Ministry of Education and Science of the Republic of Serbia (grant OI171002), Swiss Nationalfonds Foundation (grant 200020117913/1), the IN2P3-CNRS (France) and the Fermi National Accelerator Laboratory (Fermilab), a U.S. Department of Energy, Office of Science, HEP User Facility. Fermilab is managed by Fermi Research Alliance, LLC (FRA), acting under Contract No. DE-AC02-07CH11359.

References

- [1] M. Gell-Mann *Phys. Lett.* **8** (1964) 214–215.
- [2] H. Hogaasen and P. Sorba *Nucl. Phys.* **B145** (1978) 119–140.
- [3] D. Strottman *Phys. Rev.* **D20** (1979) 748–767.
- [4] C. Roiesnel *Phys. Rev.* **D20** (1979) 1646.
- [5] M. Chemtob *Nucl. Phys.* **B256** (1985) 600–608.
- [6] M. Praszalowicz *Phys. Lett.* **B575** (2003) 234–241, [arXiv:hep-ph/0308114](#) [[hep-ph](#)].
- [7] D. Diakonov, V. Petrov, and M. V. Polyakov *Z. Phys.* **A359** (1997) 305–314, [arXiv:hep-ph/9703373](#) [[hep-ph](#)].
- [8] R. L. Jaffe and F. Wilczek *Phys. Rev. Lett.* **91** (2003) 232003, [arXiv:hep-ph/0307341](#) [[hep-ph](#)].

- [9] T. Liu, Y. Mao, and B.-Q. Ma *Int. J. Mod. Phys. A* **29** no. 13, (2014) 1430020, [arXiv:1403.4455 \[hep-ex\]](#).
- [10] T. Nakano *et al.*, [LEPS Collab.] *Phys. Rev. Lett.* **91** (2003) 012002, [arXiv:hep-ex/0301020 \[hep-ex\]](#).
- [11] Y.-R. Liu, H.-X. Chen, W. Chen, X. Liu, and S.-L. Zhu *Prog. Part. Nucl. Phys.* **107** (2019) 237–320, [arXiv:1903.11976 \[hep-ph\]](#).
- [12] C. Alt *et al.*, [NA49 Collab.] *Phys. Rev. Lett.* **92** (2004) 042003, [arXiv:hep-ex/0310014 \[hep-ex\]](#).
- [13] K. T. Knoepfle, M. Zavertyaev, and T. Zivko, [HERA-B Collab.] *J. Phys.* **G30** (2004) S1363–S1366, [arXiv:hep-ex/0403020 \[hep-ex\]](#).
- [14] S. Chekanov *et al.*, [ZEUS Collab.] *Phys. Lett.* **B610** (2005) 212–224, [arXiv:hep-ex/0501069 \[hep-ex\]](#).
- [15] R. Aaij *et al.*, [LHCb Collab.] *Phys. Lett.* **B784** (2018) 101–111, [arXiv:1804.09617 \[hep-ex\]](#).
- [16] R. Aaij *et al.*, [LHCb Collab.] *Phys. Rev. Lett.* **122** no. 22, (2019) 222001, [arXiv:1904.03947 \[hep-ex\]](#).
- [17] N. Abgrall *et al.*, [NA61/SHINE Collab.] *JINST* **9** (2014) P06005, [arXiv:1401.4699 \[physics.ins-det\]](#).
- [18] A. Aduszkiewicz *et al.*, [NA61/SHINE Collab.] *Eur. Phys. J.* **C77** no. 10, (2017) 671, [arXiv:1705.02467 \[nucl-ex\]](#).
- [19] W. Press, S. Teukolsky, W. Vetterling, and B. Flannery, *Numerical Recipes in FORTRAN: The Art of Scientific Computing*. Cambridge University Press, 2nd ed., 1992.
- [20] M. Tanabashi *et al.*, [Particle Data Group Collab.] *Phys. Rev. D* **98** (Aug, 2018) 030001. <https://link.aps.org/doi/10.1103/PhysRevD.98.030001>.

The NA61/SHINE Collaboration

A. Aduszkiewicz¹⁵, E.V. Andronov²¹, T. Antičić³, V. Babkin¹⁹, M. Baszczyk¹³, S. Bhosale¹⁰, A. Blondel^{4,23}, M. Bogomilov², A. Brandin²⁰, A. Bravar²³, W. Bryliński¹⁷, J. Brzychczyk¹², M. Buryakov¹⁹, O. Busygina¹⁸, A. Bzdak¹³, H. Cherif⁶, M. Ćirković²², M. Csanad⁷, J. Cybowska¹⁷, T. Czopowicz^{9,17}, A. Damyanova²³, N. Davis¹⁰, M. Deliyergiyev⁹, M. Deveaux⁶, A. Dmitriev¹⁹, W. Dominik¹⁵, P. Dorosz¹³, J. Dumarchez⁴, R. Engel⁵, G.A. Feofilov²¹, L. Fields²⁴, Z. Fodor^{7,16}, A. Garibov¹, M. Gaździcki^{6,9}, O. Golosov²⁰, V. Golovatyuk¹⁹, M. Golubeva¹⁸, K. Grebieszko¹⁷, F. Guber¹⁸, A. Haesler²³, S.N. Igolkin²¹, S. Ilieva², A. Ivashkin¹⁸, S.R. Johnson²⁵, K. Kadija³, N. Kargin²⁰, E. Kashirin²⁰, M. Kiełbowicz¹⁰, V.A. Kireyeu¹⁹, V. Klochko⁶, V.I. Kolesnikov¹⁹, D. Kolev², A. Korzenev²³, V.N. Kovalenko²¹, S. Kowalski¹⁴, M. Koziel⁶, A. Krasnoperov¹⁹, W. Kucewicz¹³, M. Kuich¹⁵, A. Kurepin¹⁸, D. Larsen¹², A. László⁷, T.V. Lazareva²¹, M. Lewicki¹⁶, K. Łojek¹², B. Łysakowski¹⁴, V.V. Lyubushkin¹⁹, M. Maćkowiak-Pawłowska¹⁷, Z. Majka¹², B. Maksiak¹¹, A.I. Malakhov¹⁹, A. Marcinek¹⁰, A.D. Marino²⁵, K. Marton⁷, H.-J. Mathes⁵, T. Matulewicz¹⁵, V. Matveev¹⁹, G.L. Melkumov¹⁹, A.O. Merzlaya¹², B. Messerly²⁶, Ł. Mik¹³, S. Morozov^{18,20}, S. Mrówczyński⁹, Y. Nagai²⁵, M. Naskręt¹⁶, V. Ozvenchuk¹⁰, V. Paolone²⁶, O. Petukhov¹⁸, R. Płaneta¹², P. Podlaski¹⁵, B.A. Popov^{19,4}, B. Porfy⁷, M. Posiadała-Zezula¹⁵, D.S. Prokhorova²¹, D. Pszczel¹¹, S. Puławski¹⁴, J. Puzović²², M. Ravonel²³, R. Renfordt⁶, D. Röhrich⁸, E. Rondio¹¹, M. Roth⁵, B.T. Rumberger²⁵, M. Rumyantsev¹⁹, A. Rustamov^{1,6}, M. Rybczynski⁹, A. Rybicki¹⁰, A. Sadovsky¹⁸, K. Schmidt¹⁴, I. Selyuzhenkov²⁰, A.Yu. Seryakov²¹, P. Seyboth⁹, M. Słodkowski¹⁷, P. Staszal¹², G. Stefanek⁹, J. Stepaniak¹¹, M. Strikhanov²⁰, H. Ströbele⁶, T. Šušar³, A. Taranenko²⁰, A. Tefelska¹⁷, D. Tefelski¹⁷, V. Tereshchenko¹⁹, A. Toia⁶, R. Tsenov², L. Turko¹⁶, R. Ulrich⁵, M. Unger⁵, F.F. Valiev²¹, D. Veberič⁵, V.V. Vechernin²¹, A. Wickremasinghe^{24,26}, Z. Włodarczyk⁹, O. Wyszynski¹², E.D. Zimmerman²⁵, and R. Zwaska²⁴

¹ National Nuclear Research Center, Baku, Azerbaijan

² Faculty of Physics, University of Sofia, Sofia, Bulgaria

³ Ruđer Bošković Institute, Zagreb, Croatia

⁴ LPNHE, University of Paris VI and VII, Paris, France

⁵ Karlsruhe Institute of Technology, Karlsruhe, Germany

⁶ University of Frankfurt, Frankfurt, Germany

⁷ Wigner Research Centre for Physics of the Hungarian Academy of Sciences, Budapest, Hungary

⁸ University of Bergen, Bergen, Norway

⁹ Jan Kochanowski University in Kielce, Poland

¹⁰ Institute of Nuclear Physics, Polish Academy of Sciences, Cracow, Poland

¹¹ National Centre for Nuclear Research, Warsaw, Poland

¹² Jagiellonian University, Cracow, Poland

¹³ AGH - University of Science and Technology, Cracow, Poland

¹⁴ University of Silesia, Katowice, Poland

¹⁵ University of Warsaw, Warsaw, Poland

¹⁶ University of Wrocław, Wrocław, Poland

¹⁷ Warsaw University of Technology, Warsaw, Poland

¹⁸ Institute for Nuclear Research, Moscow, Russia

¹⁹ Joint Institute for Nuclear Research, Dubna, Russia

²⁰ National Research Nuclear University (Moscow Engineering Physics Institute), Moscow, Russia

²¹ St. Petersburg State University, St. Petersburg, Russia

²² University of Belgrade, Belgrade, Serbia

- ²³ University of Geneva, Geneva, Switzerland
- ²⁴ Fermilab, Batavia, USA
- ²⁵ University of Colorado, Boulder, USA
- ²⁶ University of Pittsburgh, Pittsburgh, USA